

## Evaluation of the impact of tool geometry on thrust force and bearing strength of ramie woven composite

Sri Chandrabakty, Muhammad Syaiful Fadly\*, Muchsin and I Putu Hendra

Department of Mechanical Engineering, Faculty of Engineering, Universitas Tadulako, Palu, 94148, Indonesia

Received 8 March 2025  
Revised 16 May 2025  
Accepted 11 June 2025

### Abstract

This research evaluates the impact of tool geometry on thrust force, bearing strength, and failure modes in ramie woven composite materials. Four types of tool geometries were tested: Brad and Spur Drill (BSD), Twist Drill (TWD), End Mill Centre Cut (ECC), and End Mill Centre Hole (ECH). The thrust force measurement results show that the ECC device generated the highest thrust force of 148.17 N with the lowest bearing strength of 78.00 MPa. Conversely, the lowest thrust force was observed in the TWD device at 60.52 N, which coincided with the highest bearing strength of 98.54 MPa. This condition indicates that materials with higher bearing strength tend to be stiffer, reducing the amount of thrust force that can be effectively transferred. The failure modes observed after the bearing tests indicated that all specimens experienced net tension, with damage variations depending on the tool geometry used. These results directly benefit industries utilizing ramie composites, such as the automotive, aerospace, and environmentally friendly manufacturing sectors. By reducing material damage during the machining process and improving mechanical efficiency, this research can help enhance final product quality, extend components' service life, and reduce production costs.

**Keywords:** Composite, Ramie, Woven fiber, Thrust force, Bearing strength, Drilling

### 1. Introduction

Ramie (*Boehmeria nivea*) is a perennial plant that thrives in tropical climates. It is commonly found in Japan, India, and Malaya, where it is sometimes extensively cultivated. It is also recorded in scattered locations such as Queensland, Mauritius, and Cameroon. Outside these regions, it has been naturalized or locally established in smaller islands of the West Indies, Mexico, the southern United States, Southern Europe, and continental Africa [1-3].

Ramie fibers have several unique properties that distinguish them from others. Treated ramie has high tensile strength, absorbs water well, and effectively removes moisture and bacteria from the body [4, 5]. It is resistant to sudden temperature changes, water, and bacteria. Among natural fibers, ramie ranks second only to silk and is lighter than synthetic fibers. Additionally, ramie is environmentally friendly [6]. Due to their high specific strength and stiffness-to-weight ratio, composites are now widely used as a material of choice in many engineering applications [7, 8]. In general, composites are macro-level materials that combine two or more components of different compositions, with distinct and immiscible phases that are closely bonded together [9].

Machining laminated composite materials remain complex for several reasons, including high specific stiffness, brittleness, anisotropic properties, non-homogeneity, and low thermal conductivity [10]. These factors affect machining quality, potentially resulting in tearing, defects, poor surface finish, and high tool wear. To achieve optimal machining quality, accurate and precise predictions of parameters such as cutting force, cutting speed, and feeding rate are essential. The drilling parameters must be appropriately controlled to ensure good performance, including a smooth surface finish, high-quality drilled holes, dimensional workpiece accuracy, minimal tool wear, and efficient chip removal [11, 12]. Additionally, these parameters should meet economic criteria, such as low production costs and high productivity [13].

Unlike torque, thrust force is an axial load that acts along the linear axis toward the feed rate, pushing on the drill bit [14]. This thrust force is applied perpendicular to the cutting forces and is transmitted to the test specimen during drilling. Since spindle speed is the only parameter that can be varied directly and influences feed rate, it is the most critical factor affecting thrust force during drilling [15]. Seif et al. [11] specifically investigated the effect of drilling parameters and delamination on the bearing strength of Neat GFRP and hybrid GFRP/aluminium composites. The highest bearing strength was observed in NG specimens, with levels 9.6% and 8.7% higher than those of the AG and GA specimens, respectively.

Seif et al. [16] investigated the influence of drilling parameters on the quality of holes in hybrid composite materials composed of neat glass fiber (NG) and hybrid glass fiber/Al wire mesh. The results revealed that push-out delamination was more pronounced than peel-up delamination across all specimens. Regarding circularity, the optimal parameters were a spindle speed of 3000 rpm, a feed rate of 20 mm/min, and a drill point angle of 90°. At 3000 rpm, the circularity was reduced by 83.5% compared to 1000 rpm and by 76.5% compared to 2000 rpm. A separate study examined the application of abrasive waterjet drilling (AWJD) on different GF/Al mesh hybrid composites, focusing on key parameters such as jet pressure, standoff distance, and traverse speed, and their impact on material

\*Corresponding author.

Email address: msfadly@untad.ac.id

doi: 10.14456/easr.2025.43

removal rate, hole taper ratio, and roundness error [17]. Higher cutting speeds and lower feed rates have enhanced the hole quality in CFRPs. Optimizing process parameters, designing suitable tool geometries and materials, and creating the right cutting conditions are essential to minimize drilling damage [18]. The geometry and material composition of tools are critical factors influencing the trimming quality of CFRP materials and the performance of the tools. Moreover, careful management of tool wear and failures is necessary to maintain the high cutting efficiency of tools used for CFRP trimming [19].

Bearing strength is influenced by various factors, including material type, fiber composition, layer thickness, and fiber orientation within the composite material [20, 21]. Drilling parameters such as spindle speed, feed rate, and drill bit point angle are also crucial in determining bearing strength [22]. Drilling-induced damages are affected by several key factors, including the type and design of the drill bit, cutting speed, feed rate, and support strategies. These parameters play a critical role in the machining process's overall performance and the quality of the drilled hole. Proper control of these factors can enhance hole quality, thereby improving the bearing strength of the bolt connection, as shown by Khashaba and El-Keran [23]. The drill's cutting angle significantly impacts delamination, directly affecting the drilling thrust force. A drill with a larger cutting angle tends to generate higher forces, which can lead to increased delamination. Therefore, a smaller cutting angle is generally preferred to minimize these forces and reduce delamination [24, 25].

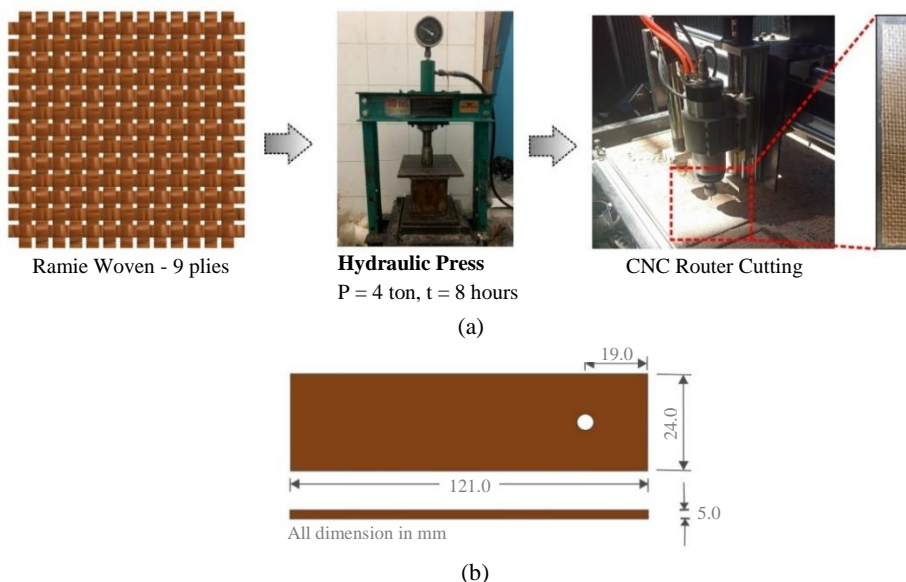
Numerous studies have examined various drilling parameters to reduce delamination and enhance hole quality. However, there is limited research on how different tool geometries impact thrust force and bearing strength in ramie woven composites, a relatively new material increasingly used in industries like automotive and aerospace. Most previous studies have concentrated on traditional materials such as metals and plastics, with few addressing the specific challenges posed by composite materials like ramie woven composites. Existing literature has not adequately explored the effects of tool geometries, such as brad and spur drill, twist drill, end mill center cut, and end mill center hole, on the mechanical properties and failure mechanisms of these composites. This research fills that gap by systematically evaluating how tool geometries influence key factors like thrust force, delamination, bearing strength, and failure microstructure in ramie woven composites. This study provides crucial insights to optimize the drilling and machining processes for ramie woven composites, enhancing material performance and utilization by offering a comparative analysis of tool geometries. Ultimately, this research seeks to address fundamental technical challenges and make significant practical contributions to the composite materials industry. Different types of drill bits, including conventional and end mill styles, were assessed to determine their impact on drilling efficiency and induced damage in the material. Moreover, a direct correlation between machining parameters, particularly thrust force, and the resulting bearing strength of the drilled joints was established an aspect seldom explored in studies on natural fiber composites. The outcomes of this work provide valuable recommendations for improving drilling techniques to reduce damage and enhance the mechanical integrity of sustainable composite joints.

## 2. Materials and experimental

### 2.1 Specimen fabrication

The ramie sheets were cut to match the mold size of 20x20 cm. Each sheet of ramie fiber weighs an average of 9.42 grams. The specimen to be molded has a volume of 200 cm<sup>3</sup> (length = 20 cm, width = 20 cm, and thickness = 0.5 cm). A 30% volume fraction of hybrid fiber (60 cm<sup>3</sup>) was used to mold one composite panel, requiring nine sheets of woven ramie with a total weight of 84.78 grams (55.78 cm<sup>3</sup>). The composite binder was Yukalac 157 BQTN-EX polyester resin, with MEKPO catalyst as the hardener. The amount of MEKPO catalyst mixed with the polyester resin was 1% of the resin volume.

The specimen molding is performed using the hand lay-up technique. The first three ramie sheets are placed into the mold, which is lined with plastic, and a small amount of resin is poured and evenly spread. This process is repeated until the final ramie fiber sheet is placed. The mold is then closed and subjected to 4 tons of pressure using a press machine, and left for 8 hours to ensure the material adheres and dries completely. The mold is opened after the 8-hour curing process, and the specimen is shaped using a CNC Router Cutting machine. The specimen manufacturing process is illustrated in Figure 1. The ramie fibers used were in the form of plain weave fabric. This study conducted nine trials per sample, ensuring good repeatability and reducing the impact of existing fiber variations. The material preparation process was also standardized, and all samples were treated with the same method to ensure consistency in the experimental conditions.

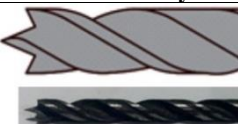
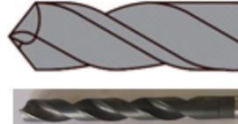
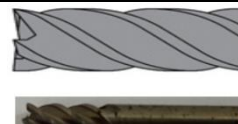


**Figure 1** Manufacturing ramie woven composites

## 2.2 Drilling process

The specimen drilling process is conducted using a Sinumerik 808D CNC milling machine. Four drill bits are selected: twist drill, brad/spur drill, and end mill center cutting, and end mill center hole. The drilling parameters follow the previous reference, with a spindle speed of 1500 RPM and a feed rate of 0.10 mm/rotation [15]. Table 1 shows the geometries of the tools used for testing. Figure 2 shows the details of the drill bit geometry.

**Table 1** Tool drill geometries

Tool Geometry	Configuration	Code
	Brad and Spur Drill	BSD
	Twist Drill	TWD
	End Mill Centre Cut	ECC
	End Mill Centre Hole	ECH

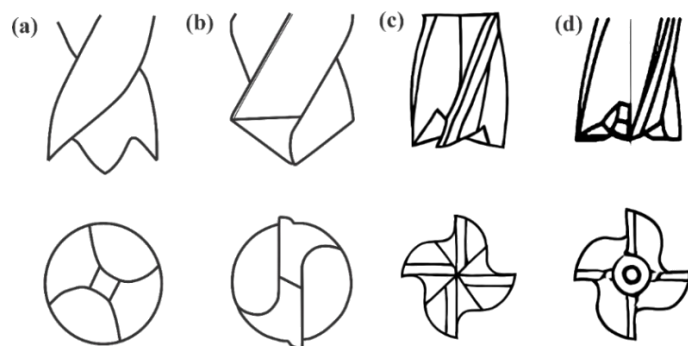


**Figure 2** Drill geometry: (a) BSD, (b) TWD, (c) ECC, (d) ECH

During the drilling process, thrust force is measured using a dynamometer sensor equipped with a load cell with a maximum capacity of 15 kg, positioned beneath the specimen. The drilling process is illustrated in Figure 3. The data generated by the sensor is transmitted to a computer, where MakerPlot software is used to read and record the thrust force data (Figure 4). A dynamometer was positioned directly beneath the specimen to measure the axial force generated during drilling. This device, integrated with a load cell (15 kg capacity), was connected to a data acquisition system that continuously logged force readings throughout the drilling process. Calibration was conducted beforehand to maintain the accuracy of the measurements.

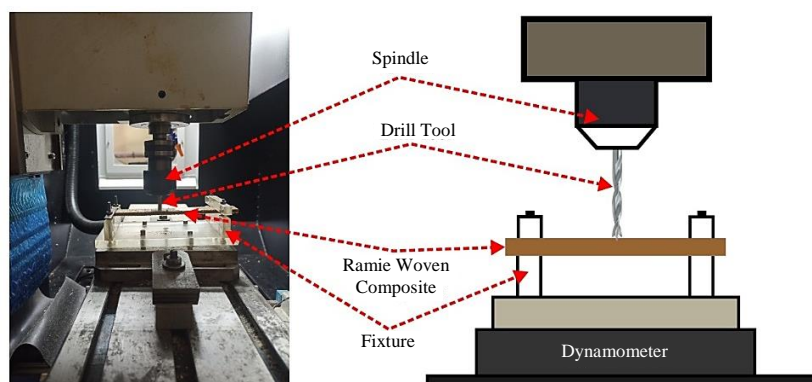


**Figure 3** Experimental setup for the CNC drilling process

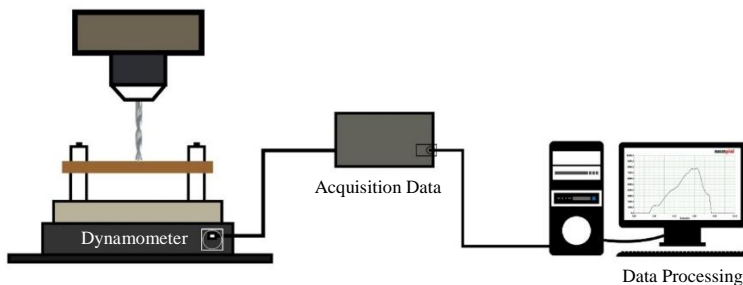


**Figure 4** Experimental setup for evaluating thrust force

The delamination factor is determined using a straightforward one-dimensional equation, which is commonly employed in the field, as outlined by Khashaba [26] in Eq. (1). In this equation, representing  $D_m$  is the maximum diameter of the delamination zone and  $D_o$  is the drill bit diameter, as shown in Figure 5.

$$F_d = \frac{D_m}{D_o} \quad (1)$$

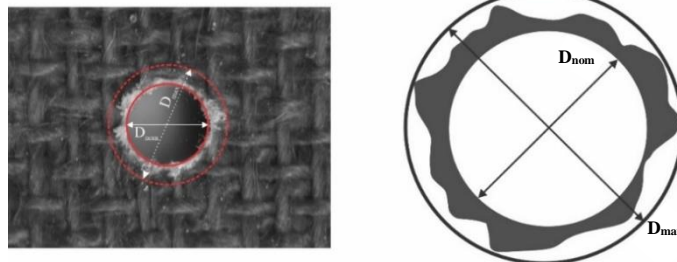


**Figure 5** Measurement of delamination

### 2.3 Bearing test

Bearing strength testing is conducted to determine the impact of tool geometry on the damage and tensile strength of ramie fiber composite materials. This testing follows the ASTM D953-02 standard (Standard Test Method for Bearing Strength of Plastics) using a hydraulic universal testing machine, as shown in Figure 6. Each specimen, featuring a centrally located drilled hole, was positioned on a specially designed fixture configured for single-shear loading. A steel loading pin was inserted into the hole, and compressive force was gradually applied using a universal testing machine (UTM) operated at a fixed crosshead speed. The fixture was engineered to maintain accurate alignment throughout the test, minimizing unintended bending effects. The loading process continued until visible signs of damage or failure occurred. The bearing strength was then determined by identifying the peak load carried by the specimen before failure.

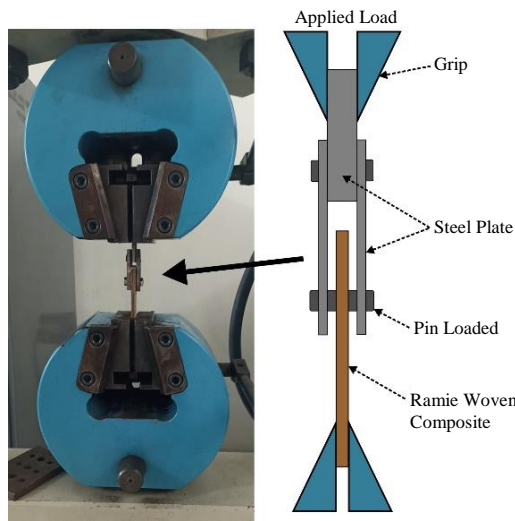


**Figure 6** Experimental setup for the bearing strength test

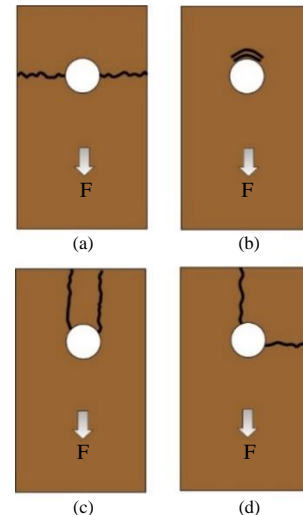


**Figure 7** Failure modes of mechanically fastened composite joints

The failure modes in composites with mechanically fastened joints can be classified into four types [27-29]: net-tension (a), shear-out (b), bearing, and cleavage, as shown in Figure 7. According to Eq. 2, the bearing strength is calculated by dividing the maximum load that a structure can bear at failure by the contact area [11, 30]. In this equation,  $F_{max}$  represents the maximum applied force,  $D_h$  is the hole diameter, and  $t$  is the part thickness.

$$\sigma_b = \frac{F_{max}}{D_h \times t} \quad (2)$$

### 3. Results and discussion

#### 3.1 Thrust force

Figure 8 shows the complete drilling cycle on ramie woven composite material using variations in tool geometries: BSD, TWD, ECC, and ECH. The drilling process consists of four stages, as illustrated in Figure 8(a). Stage I begins when the drill bit tip touches the workpiece surface and continues until the cutting 'spur' tip penetrates the upper layer of the test specimen. Stage II occurs when the drill bit penetrates the matrix and reaches the ramie woven layer, with a relatively stable thrust force.

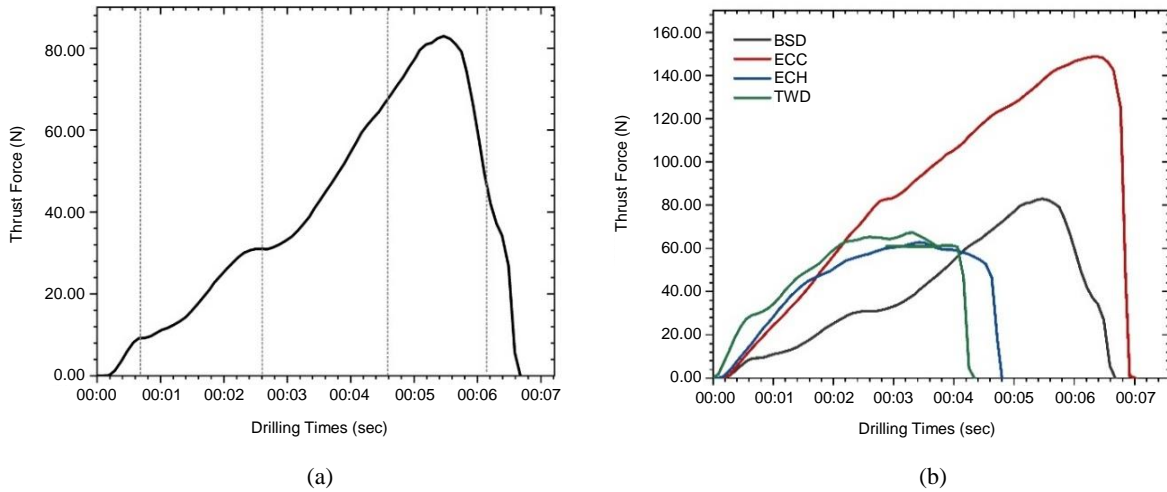
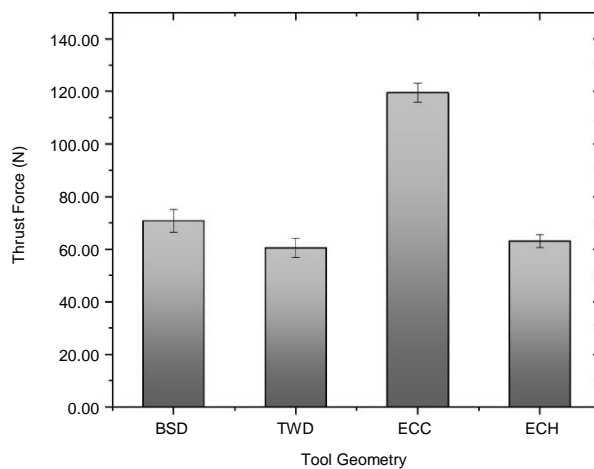


**Figure 8** Thrust force during the drilling cycle: (a) single drilling operation, (b) tool geometry variables

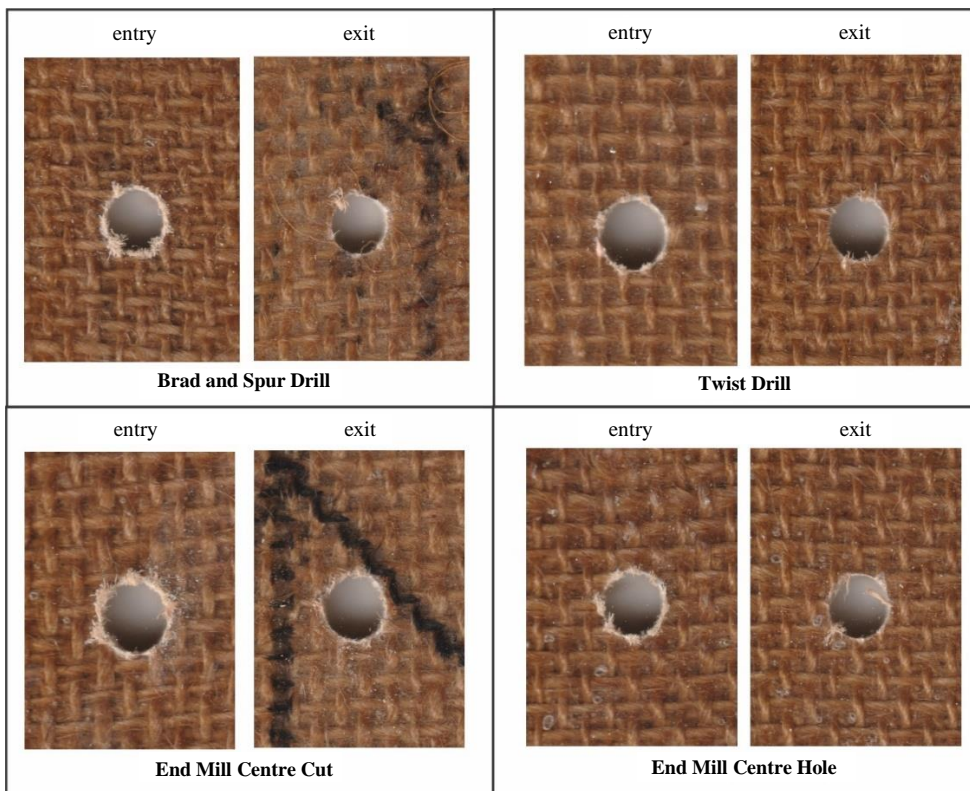
Stage III occurs when the brad-point tip penetrates the ramie woven layer, while the spear point cuts through the layer to ensure the desired hole diameter. During this stage, the thrust force reaches its peak. Stage IV occurs when the drill bit penetrates the final layer of the workpiece, leading to the reaming process, during which the thrust force drastically decreases to zero. Figures 8(b) and seven show that the ECC drill bit generates the highest thrust force compared to the others, reaching a peak of 148.17 N at 0.067 seconds. This is attributed to the ECC geometry, which has a sharper bit tip and a larger contact surface, resulting in greater friction during drilling [31]. With its slimmer tip, the ECH drill bit exhibits a lower thrust force, peaking at 62.65 N at 0.065 seconds, due to the reduced contact area and friction. The TWD and BSD drill bits display lower and more stable thrust forces, with TWD peaking at around 67.27 N and BSD at around 82.91 N.

Separate research by Chandrabakty et al. [15] examined how machining parameters impact four varying drill bit diameters when applied to ramie woven composites reinforced with an unsaturated polyester matrix. Their findings revealed that the duration of drilling influences the magnitude of thrust generated. Specifically, increasing the feed rate leads to a reduction in drilling duration. Additionally, it was noted that larger drill bit diameters are closely associated with a notable rise in thrust force during the operation [15]. Latha et al. [32] showed that the drill bit geometry significantly affects the thrust force and delamination in GFRP composites, indicating that a sharper point angle can reduce the thrust force.

This phenomenon can be explained by the geometric design of these drill bits, which reduces resistance during the drilling of composite materials, thereby decreasing heat accumulation and friction. According to Shetty et al. [33], thrust force can enhance hardness, wear resistance, thermal conductivity, and heat dissipation from the drill bit. These factors help reduce the heat generated by the contact between the drill bit tip and the material, thereby lowering friction.

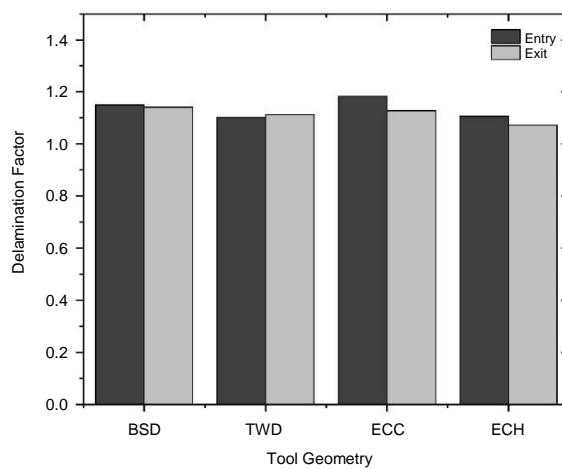


**Figure 9** The relationship between thrust force and tool geometry



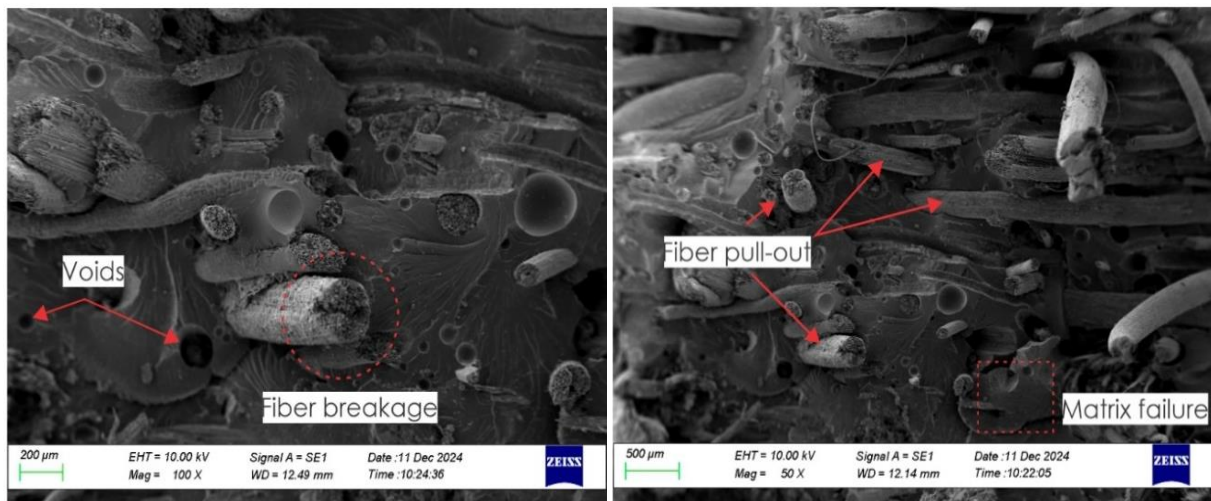
**Figure 10** Schematic illustrations of the types of delamination

Figure 9 shows the end mill centre cut, which generates a high thrust force due to its larger cutting edge. Consequently, various failure mechanisms can be observed during the drilling of ramie woven composite, as illustrated in Figure 10, which causes greater material displacement and increases the stress between the composite layers, leading to delamination. Elevated thrust force leads to increased mechanical stress at the tool-material interface, resulting in faster abrasive wear of the drill bit and fiber-matrix separation (delamination) and surface imperfections within the ramie woven composite. Such damage compromises both the material's strength and its overall structural integrity. Two types of delamination, namely peel-up and push-out, were observed while drilling the three specimen components [34]. On the entry side, delamination is evident around the hole due to the thrust force generated by the drill bit, leading to incomplete fiber cutting (uncut fiber). On the exit side, a push-out zone can be observed, where fibers and the matrix are displaced due to insufficient cutting efficiency, resulting in a rough and uneven hole surface. This type of failure is common in composite drilling due to the material's heterogeneous structure, which makes it susceptible to delamination and fiber tearing caused by mechanical interactions with the drill bit. The average delamination factor values are shown in Figure 11.



**Figure 11** Effect of tool geometry on delamination factor

Figure 11 illustrates that ECC generates the most significant variation in delamination between the entry and exit holes. BSD shows a 2.78% reduction in delamination compared to the ECC specimen. The ECC specimen also exhibits a significant increase in peeling and push-out force ( $F_a$ ) compared to other configurations. According to Kilickap et al. [35], as the thrust force increases, the stress on the material intensifies, particularly at the interface between the layers of composite materials. This heightened stress can cause the layers to separate, increasing the delamination factor [35].



**Figure 12** The structural characteristics of a drilled hole in composite materials

Figure 12 shows the SEM images, which reveal several types of damage, including voids, fibre breakage, fibre pull-out, and matrix failure. The presence of voids indicates imperfections within the composite structure, which can weaken its mechanical properties. Fiber breakage and pull-out suggest that the drilling process causes excessive stress on the fibers, leading to their detachment from the matrix. Additionally, matrix failure highlights the inability of the resin to withstand the cutting forces, resulting in cracks and material fragmentation. These defects contribute to poor hole quality, reducing the structural integrity and performance of the composite material in practical applications.

The surface may become rougher during the drilling process due to various cutting mechanisms. The matrix material fails under high pressure, while fragmented parts of the matrix adhere to the cut areas. Cracks in the matrix are visible on the surface due to the high pressure exerted during tool penetration. Additionally, elevated temperatures cause the matrix to melt and adhere to the walls of the cut surface. The high drilling force also causes fibers to be pulled out, protrude, and detach from the matrix. In some areas, the fibers break and fragment.

### 3.2 Bearing strength

According to Figure 13, the TWD exhibits the highest bearing strength at 98.54 MPa, indicating that the twist drill geometry provides more uniform stress distribution and more efficient penetration during drilling, thereby reducing damage to the ramie woven composite. The BSD also shows relatively high bearing strength, slightly less than the TWD, which can be attributed to its design, which reduces delamination and edge damage. The ECH, on the other hand, has a lower bearing strength than the BSD and TWD but higher than the ECC due to its ability to reduce the magnitude of thrust force, though it is not as efficient as the TWD in stress distribution. Finally, the ECC displays the lowest bearing strength, likely due to less uniform stress distribution, resulting in greater damage to the ramie woven composite during drilling.

The study conducted by Seif et al. [11] emphasized that delamination around the drilled hole plays a crucial role in reducing the specimen's bearing strength. As the delamination factor increases, the bearing strength correspondingly decreases, indicating a direct negative impact of delamination on the material's load-bearing capacity [11]. Khashaba and El-Keran [23], research indicates that the feed rate significantly influences bearing strength, where a lower feed rate combined with higher spindle speed tends to improve the material's ability to withstand bearing loads.

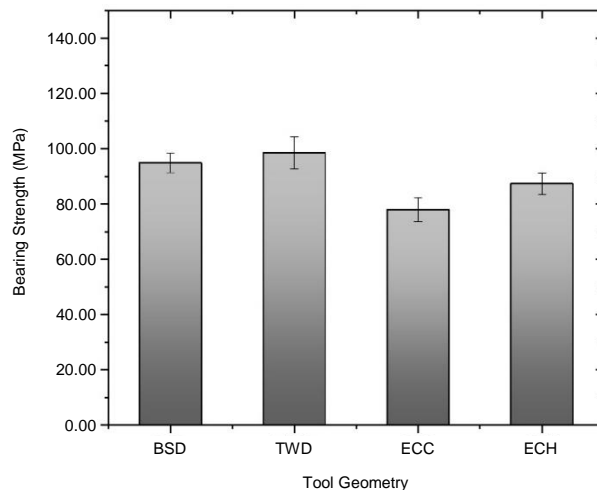


**Figure 13** Bearing strength for each type of geometry tool

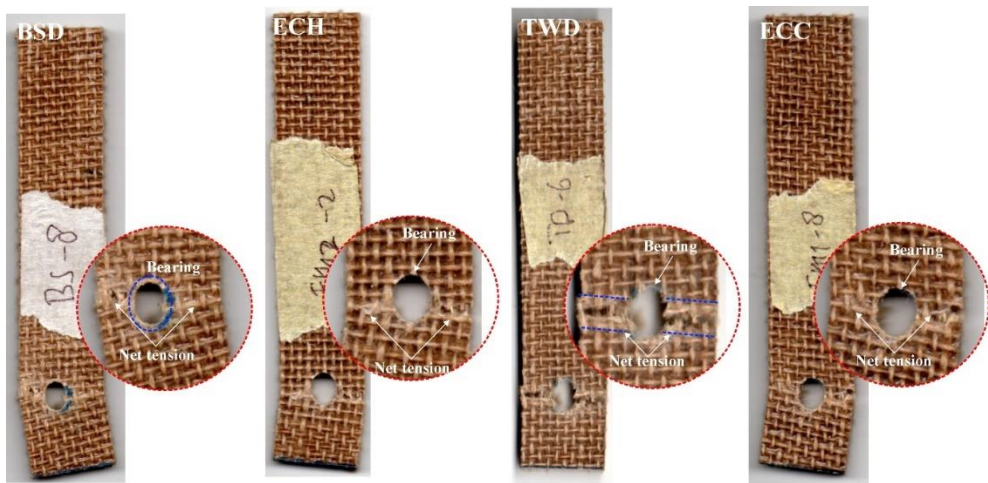


**Figure 14** Failure modes after bearing tests

Figure 14 shows that all specimens exhibit a net tension failure mode, characterised by significant damage around the hole. Substantial tearing and delamination are observed in specimens drilled with BSD and TWD. In contrast, specimens drilled with ECH and ECC show less damage but still fall within the net tension category. This failure mode occurs due to the stress accumulated around the drilled hole, causing the composite material to experience significant structural damage in that area. Kim et al. [30], explained that mechanically fastened joints can exhibit various failure mechanisms, such as net-tension failure, shear-out, cleavage, and bearing failure. Bearing failure is primarily characterized by several damage mechanisms, including micro-buckling of fibers, cracks forming in the matrix, separation between layers (delamination), and shear cracks occurring out of the material's plane [36].

#### 4. Conclusions

1. The shape of the tool geometry has a notable influence on the thrust force generated during machining. ECC recorded the highest thrust force among the tested geometries at 119.49 N, while TWD resulted in the lowest, at 60.52 N. This indicates a significant increase of 58.97 N when using the ECC tool compared to TWD. The BSD and ECH geometries produced thrust forces of 70.75 N and 63.01 N, respectively. The elevated thrust force observed with the ECC design is likely due to its structural features, which may increase cutting resistance due to a larger contact area or less favorable cutting angles.
2. The highest bearing strength was obtained with TWD at 98.54 MPa, followed by BSD at 94.89 MPa, while the lowest value was recorded with ECC at 78.00 MPa. Compared to ECC, the bearing strength increased by approximately 26.33% with TWD, while BSD and ECH showed increases of 21.65% and 12%, respectively. ECC generates a higher thrust force, which tends to increase damage around the hole edge, reducing joint strength.
3. Morphological analysis of the drilled specimens showed fiber pull-out and matrix failure around the hole area. Regarding bearing strength, all specimens failed through a mixed mode of bearing and net-tension failure.

#### 5. Acknowledgements

The author wishes to express his sincere appreciation to the Department of Mechanical Engineering, Faculty of Engineering, Universitas Tadulako.

#### 6. References

- [1] Rehman M, Fahad S, Saleem MH, Hafeez M, UR Rahman MH, Liu F, et al. Red light optimized physiological traits and enhanced the growth of ramie (*Boehmeria nivea* L.). *Photosynthetica*. 2020;58(4):922-31.
- [2] Kandimalla R, Kalita S, Choudhury B, Devi D, Kalita D, Kalita K, et al. Fiber from ramie plant (*Boehmeria nivea*): a novel suture biomaterial. *Mater Sci Eng C*. 2016;62:816-22.
- [3] Luan MB, Jian JB, Chen P, Chen JH, Chen JH, Gao Q, et al. Draft genome sequence of ramie, *Boehmeria nivea* (L.) Gaudich. *Mol Ecol Resour*. 2018;18(3):639-45.
- [4] Ren Y, Wei Q, Lin L, Shi L, Cui Z, Li Y, et al. Physicochemical properties of a new starch from ramie (*Boehmeria nivea*) root. *Int J Biol Macromol*. 2021;174:392-401.
- [5] Murali B, Vijaya Ramnath B, Chandramohan D. Mechanical properties of *Boehmeria nivea* reinforced polymer composite. *Mater Today: Proc*. 2019;16:883-8.
- [6] Lubis MAR, Aristri MA, Sari RK, Iswanto AH, Al-Edrus SSO, Sutiawan J, et al. Isocyanate-free tannin-based polyurethane resins for enhancing thermo-mechanical properties of ramie (*Boehmeria nivea* L.) fibers. *Alex Eng J*. 2024;90:54-64.
- [7] Fadly MS, Bakri B, Anwar K, Chandrabakty S, Mustafa, Naharuddin, et al. Evaluation of projectile penetration position on perforated plate on ballistic resistance of composite sandwich panels. *IOP Conf Ser: Earth Environ Sci*. 2023;1157:012033.
- [8] Fadly MS, Purnowidodo A, Setyarini PH, Bakri B, Chandrabakty S. Perforation and penetration of fiber metal laminates target by hemispherical projectile. *Int J Mech Eng Technol Appl*. 2023;4(2):190-7.
- [9] Hull D, Clyne TW. An introduction to composite materials. 2<sup>nd</sup> ed. Cambridge: Cambridge university press; 2012.
- [10] Jagadeesh P, Rangappa SM, Suyambulingam I, Siengchin S, Puttegowda M, Binoj JS, et al. Drilling characteristics and properties analysis of fiber reinforced polymer composites: a comprehensive review. *Heliyon*. 2023;9(3):e14428.

- [11] Seif A, Fathy A, Megahed AA. Effect of drilling process parameters on bearing strength of glass fiber/aluminum mesh reinforced epoxy composites. *Sci Rep.* 2023;13(1):12143.
- [12] Straznicky PV, Laliberté JF, Poon C, Fahr A. Applications of fiber-metal laminates. *Polym Compos.* 2000;21(4):558-67.
- [13] Li Y, She L, Wen L, Zhang Q. Sensitivity analysis of drilling parameters in rock rotary drilling process based on orthogonal test method. *Eng Geol.* 2020;270:105576.
- [14] Bolat Ç, Karakılçın U, Yalçın B, Öz Y, Yavaş Ç, Ergene B, et al. Effect of drilling parameters and tool geometry on the thrust force and surface roughness of aerospace grade laminate composites. *Micromachines.* 2023;14(7):1427.
- [15] Chandrabakty S, Renreng I, Djafar Z, Arsyad H. Experimental study and investigation of thrust force and delamination damage of drilled ramie woven reinforced composites. *Int J Automot Mech Eng.* 2020;17(1):7618-28.
- [16] Seif A, Sadoun AM, Fathy A, Megahed AA. Evaluation of hole quality in drilling process of GF/Aluminum wire mesh reinforced epoxy composites. *Alex Eng J.* 2024;94:257-73.
- [17] Seif A, Fathy A, El Aal MIA, Megahed AA. Optimization of AWJ parameters for improved material removal and hole geometry in drilling of Glass Fiber/Aluminum mesh epoxy hybrid composites. *Polym Compos.* 2024;45(7):6644-61.
- [18] Xu J, Geier N, Shen J, Krishnaraj V, Samsudeensadham S. A review on CFRP drilling: fundamental mechanisms, damage issues, and approaches toward high-quality drilling. *J Mater Res Technol.* 2023;24:9677-707.
- [19] Geier N, Xu J, Poór DI, Dege JH, Davim JP. A review on advanced cutting tools and technologies for edge trimming of carbon fibre reinforced polymer (CFRP) composites. *Compos B: Eng.* 2023;266:111037.
- [20] Yoon D, Kim S, Kim J, Doh Y. Study on bearing strength and failure mode of a carbon-epoxy composite laminate for designing bolted joint structures. *Compos Struct.* 2020;239:112023.
- [21] Xiao Y, Ishikawa T. Bearing strength and failure behavior of bolted composite joints (part II: modeling and simulation). *Compos Sci Technol.* 2005;65(7-8):1032-43.
- [22] Silva JM, Ferreira F, Abreu SM, Matos JE, Durão LMP. Correlation of drilling damage with mechanical strength: a geometrical approach. *Compos Struct.* 2017;181:306-14.
- [23] Khashaba UA, El-Keran AA. Drilling analysis of thin woven glass-fiber reinforced epoxy composites. *J Mater Process Technol.* 2017;249:415-25.
- [24] Li J, Zhang Y, Lin L, Zhou Y. Study on the shear mechanics of gas hydrate-bearing sand-well interface with different roughness and dissociation. *Bull Eng Geol Environ.* 2023;82(11):404.
- [25] Morkavuk S, Köklü U, Aslantaş K. An experimental comprehensive analysis of drilling carbon fiber reinforced plastic tubes and comparison with carbon fiber reinforced plastic plate. *J Reinf Plast Compos.* 2023;42(7-8):323-45.
- [26] Khashaba UA. Delamination in drilling polymeric composites: a review. In: Paulo Davim J, editor. *Drilling of composite materials.* New York: Nova Science Publishers; 2009. p. 57-81.
- [27] Osama MM, Selmy AI, Abdelhaleem AMM, Megahed AA. Comparison between bearing strengths of molded-in and machined holes of GFR/PP composites. *Sci Rep.* 2022;12(1):14756.
- [28] Yang KC, Hsu RJ, Hsu CF. Effect of end distance and bolt number on bearing strength of bolted connections at elevated temperature. *Int J Steel Struct.* 2013;13:635-44.
- [29] Može P, Beg D. A complete study of bearing stress in single bolt connections. *J Constr Steel Res.* 2014;95:126-40.
- [30] Kim DU, Seo HS, Jang HY. Study on mechanical bearing strength and failure modes of composite materials for marine structures. *J Mar Sci Eng.* 2021;9(7):726.
- [31] Pereszlai C, Geier N. Comparative analysis of wobble milling, helical milling and conventional drilling of CFRPs. *Int J Adv Manuf Technol.* 2020;106(9):3913-30.
- [32] Latha B, Senthilkumar VS, Palanikumar K. Influence of drill geometry on thrust force in drilling GFRP composites. *J Reinf Plast Compos.* 2011;30(6):463-72.
- [33] Shetty N, Herbert MA, Shetty R, Shetty DS, Vijay GS. Soft computing techniques during drilling of bi-directional carbon fiber reinforced composite. *Appl Soft Comput.* 2016;41:466-78.
- [34] Ameur MF, Habak M, Kenane M, Aouici H, Cheikh M. Machinability analysis of dry drilling of carbon/epoxy composites: cases of exit delamination and cylindricity error. *Int J Adv Manuf Technol.* 2017;88:2557-71.
- [35] Kilickap E, Çelik YH, Yenigun B. Experimental evaluation of parameters affecting delamination factor, tensile strength, thrust force and surface roughness in drilling of GFRP. *Surf Rev Lett.* 2023;30(4):2350025.
- [36] Xiao Y, Ishikawa T. Bearing strength and failure behavior of bolted composite joints (part I: experimental investigation). *Compos Sci Technol.* 2005;65(7-8):1022-31.